



HAL
open science

Advanced MRI shape analysis as a predictor of histologically aggressive supratentorial meningioma

Guillaume Friconnet, Maxime Baudouin, Waleed Brinjikji, Suzana Saleme, Victor Hugo Espíndola Ala, Marie-Paule Boncoeur-Martel, Charbel Mounayer, Aymeric Rouchaud

► To cite this version:

Guillaume Friconnet, Maxime Baudouin, Waleed Brinjikji, Suzana Saleme, Victor Hugo Espíndola Ala, et al.. Advanced MRI shape analysis as a predictor of histologically aggressive supratentorial meningioma. *Journal de Neuroradiologie / Journal of Neuroradiology*, 2021, 10.1016/j.neurad.2020.12.007 . hal-03407530

HAL Id: hal-03407530

<https://unilim.hal.science/hal-03407530v1>

Submitted on 22 Jul 2024

HAL is a multi-disciplinary open access archive for the deposit and dissemination of scientific research documents, whether they are published or not. The documents may come from teaching and research institutions in France or abroad, or from public or private research centers.

L'archive ouverte pluridisciplinaire **HAL**, est destinée au dépôt et à la diffusion de documents scientifiques de niveau recherche, publiés ou non, émanant des établissements d'enseignement et de recherche français ou étrangers, des laboratoires publics ou privés.



Distributed under a Creative Commons Attribution - NonCommercial 4.0 International License

Advanced MRI shape analysis as a predictor of histologically aggressive supratentorial meningioma

Guillaume Friconnet (MD)¹; Maxime Baudouin (MD)¹; Waleed Brinjikji (MD, PhD)²; Suzana Saleme (MD)¹; Victor Hugo Espíndola Ala (MD)¹; Marie-Paule Boncoeur-Martel (MD)¹; Charbel Mounayer (MD, PhD)^{1,3}; Aymeric Rouchaud (MD, PhD)^{1,3}

1. From the Department of Radiology, Centre Hospitalier et Universitaire Dupuytren, Limoges, France.
2. From the Department of the Department of Radiology, Mayo Clinic, Rochester, Minnesota, USA.
3. CNRS, XLIM, UMR 7252, F_87000, Limoges, France.

Correspondence to Guillaume Friconnet, MD, Department of Radiology, Centre Hospitalier et Universitaire Dupuytren, 2 avenue Martin Luther King, 87042 Limoges, France. Phone : +33(0)604022498 ; E-mail: guillaume.friconnet@yahoo.fr

Declarations of interest : none

Funding : This research did not receive any specific grant from funding agencies in the public, commercial, or not-for-profit sectors.

Advanced MRI shape analysis as a predictor of histologically aggressive supratentorial meningioma

Article type

Original research.

Keywords

Fractal Analysis; Meningioma; MR-Imaging; Neuro-Oncology; Shape Analysis;

Abbreviations

Acc = Accuracy ; AUC = Area Under Curve; FD = Fractal Dimension ; ICC = Intraclass Correlation Coefficient; NPV = Negative Predictive Value; NSB = Number of Skeleton's branches ; PPV = Positive Predictive Value; ROC = Receiver Operating Characteristic; RSL = Relative skeleton's length ; SD = Standard Deviation; Se = Sensibility; Sp = Specificity.

Word count

3486 words.

ABSTRACT

Background and purpose: A subset of aggressive meningioma is associated with higher morbidity and requires a different therapeutic management. This subset consists of World Health Organization (WHO) grade II and III meningioma, characterized particularly with microscopic brain invasion. Numerous studies tried to screen aggressive meningioma on pre-operative MRI. The objective of the study was to determine if an advanced shape analysis of supratentorial meningioma outlines could reliably predict WHO II-III grade and histological brain invasion.

Materials and Methods: We performed a retrospective analysis for all consecutive patients who underwent surgery for supratentorial histologically-proven meningioma from 2010 to 2018. Pre-operative MRI T1WI contrast enhanced axial, coronal and sagittal slices were collected from 101 patients. Advanced shape analysis including fractal analysis and topological skeleton analysis was performed. Shape analysis parameters were correlated with histopathological WHO grading and brain invasion on surgical pieces.

Results: Shape analysis features such as a low circularity, a low solidity, a high fractal dimension and a high number of skeleton's branches were significantly correlated with both WHO II-III meningioma and histological brain invasion. Cross-validated regression models including these features were predictive of WHO II-III meningioma and brain invasion with respective AUC of 0.71 and 0.72.

Conclusions: MRI shape analysis provides informative imaging biomarkers to predict high WHO grade and histological brain invasion of supratentorial meningioma. Further prospective studies including the evaluation of a fully-automatized and totally reproducible process are required to confirm the results.

I - Introduction

Meningioma are the most common primary intracranial tumors in adults[1,2]. Although mostly benign, a subset of aggressive meningiomas are associated with higher morbidity and requires a more aggressive management strategy[1,3]. Typically, aggressive meningiomas (i.e. WHO Grade II and III)[1,4] are diagnosed post-surgically according to several pathological criteria including microscopic brain invasion[2,5].

However, there is a growing interest in identifying imaging biomarkers of aggressive meningiomas[6–8]. The most common findings associated with aggressive meningiomas include irregular tumoral outlines[6,9,10]. Shape analysis provides a means to quantify the subjective concept of irregularity through numerous features[3,4].

Many studies analyzed the association between shape and meningioma aggressiveness[1,2,4,7,11]. However, these works included only a limited sample of shape features or often incorporated these features into complex radiomics models.

The objective of the present study was to determine specifically if an advanced shape analysis of supratentorial meningioma outlines could reliably predict high WHO grade and histological brain invasion.

II – Material and Methods

Patients

We performed a retrospective analysis of our database for all consecutive patients who underwent surgery for supratentorial histologically-proven meningioma from 2010 to 2018. Patients matching at least one of the following criteria have been excluded: en-plaque subtype, recurrence after previous surgery, multiples and voluminous simultaneous meningiomas. We considered that these criteria were prone to interfere with tumoral shape and therefore to bias the results.

MRI examination

MRI examinations were performed in our institution with two different systems: Achieva 3.0 T MRI (Philips, Netherlands) and Area 1.5 T MRI (Siemens, Germany). For all patients, 3D isotropic T1-gadolinium-enhanced images (Dotarem 0.5 mmol/ml : 0.01 mmol/kg IV, Guerbet) were acquired with axial, coronal and sagittal reformation. Detailed information concerning MRI protocols are provided in **Supplemental Material. Table 1**. In each plane the slice with the largest cross-section was selected. **Table 1** summarizes the studied parameters.

Standard post-processing

Post-processing was performed using ImageJ software (National Institutes of Health, Bethesda, Maryland, USA)[12]. First stage was a rescaling step using standard bicubic interpolation[13] in order to obtain for each slice a 256 x 256 px square fitted to the tumoral great axis. Pixel intensities were normalized (8-bit-grayscale). Then, images were semi-automatically binarized using the algorithm described by Huang[14] in order to obtain the tumoral area in white overwhelmed by a black background. Aberrations were manually corrected. **Figure 1** shows an example of standard post-processing.

Shape analysis

Shape analysis data were obtained on ImageJ and included circularity, aspect ratio and solidity.

Circularity was defined as $Circ = 4\pi \left(\frac{area}{perimeter^2} \right)$ with 1 indicating a perfect circle. Aspect ratio was defined as $Asp = \frac{major\ axis}{minor\ axis}$. Solidity was defined as $Sol = \frac{area}{convex\ area}$, increasing with the regularity (convex area being the area of the convex hull defined as the smallest convex set containing the original region).

Fractal analysis

Previous images underwent a supplemental edge detection processing (standard Sobel edge filter[15]) in order to extract tumoral outlines. A box-counting method was used to determine the fractal dimension (FD) for each image using FracLac plugin for ImageJ[16]. A practical limit of 3 pixels was set as a minimal box size considering the spatial resolution of MRI examination in order to avoid noise-related aberrations[16,17]. A limit of 45 % of the image size was equally applied as a maximal box size to avoid non-pertinent measures[16]. **Figure 2** presents an example of box counting.

Skeleton analysis

Skeleton analysis was automatically performed using the “Skeletonize” and “AnalyseSkeleton” plugins for ImageJ[18]. A topological skeleton is a thin version of a shape that is equidistant to its boundaries. This skeleton was obtained with the first plugin through an image-thinning process (iterative erosions based on decision-tree algorithm). The second plugin extracted the following parameters: number of skeleton’s branches (NSB) and relative skeleton length (RSL) defined by the ratio between skeleton length and the sum of major and minor axis’ lengths. **Figure 3** presents an example of topological skeleton.

Mean values

As circularity, solidity, aspect ratio, FD, NSB and RSL were extracted in the three space planes for each meningioma, the average values have been used for statistical tests.

Reliability

Each slice was selected and post-processed independently and blindly by two raters (one 10-year experienced neuroradiologist and an in-training fellow). Inter-rater variability was evaluated with intra-class correlation coefficient (ICC) according to a two-way mixed-effects model.

Visual examination

A visual analysis consisting in a semantical rating of the shape of each meningioma as “regular” or “irregular” was performed by the two same raters (blinded to the results of the computer-assisted shape analysis performed several months before). This rating was based on the 3D T1-gadolinium enhanced images, taking all the slices into consideration, in order to remain close to daily practice. Irregularity was defined as the presence of either patent spiculation or micro- / macro-lobulation.

Histopathological data.

All operative specimens were analyzed by a team of two experienced neuropathologists. The following parameters were collected: WHO grading (2016 classification), parenchymal brain invasion. Glial Fibrillary Acidic Protein-immunohistochemical staining was performed in order to assess brain invasion [19].

Statistics

Continuous variables were reported as mean \pm standard deviation (SD) and categorical variables as percentage and number. Variables were compared by using appropriate non-parametric tests due to non-normal distribution. Mean values between the two raters were used in the different comparisons. Data were analyzed using R version 3.4.0 for Windows V17.0 (R Foundation for Statistical Computing, Vienna, Austria).

Ethics

This study was approved by the Institutional Review Board (IRB) of our institution. Written informed consent was not obtained from participants because of the retrospective design of this study; therefore, the IRB of the hospital waived the need for written informed consent from participants.

III – Results

Patients

Ten patients matched the exclusion criteria : en-plaque meningioma (1 patient) ; recurrence after surgery (8 patients) ; multiples and voluminous simultaneous meningioma (1 patient). 108 meningioma were included in this study. Seven meningioma were subsequently excluded because of motion artifacts leading to non-processable images.

Mean age was 60.2 (SD: 14.5) years. Mean tumoral great axis was 51.0 (SD: 16.4) mm. Aggressive meningioma (WHO II-III) accounted for 38.6 % of the studied population (39/101). Detailed description of the population is displayed in **Table 1**.

Shape, fractal and skeleton analysis

A low circularity was significantly correlated with both histological brain invasion ($P = .0016$) and WHO II-III meningioma ($P = .00029$). An identical correlation with these two histopathological criteria was observed concerning a low solidity (respective p-values : 0.00038 and 0.0149), a high FD (respective p-values : 0.0079 and 0.00059), a high NSB (respective p-values : 0.0027 and 0.0040) and a high RSL (respective p-values : 0.00194 and 0.0177). Detailed results are presented in **Table 2**. Representative images are presented in **Figure 4**.

Reliability and correlation between extracted features

Inter-rater ICC were as follows : circularity (0.832), aspect ratio (0.974), solidity (0.770), FD (0.773), NSB (0.746) and RSL (0.326). Correlation between the extracted features is presented in **Supplemental Material. Table 2**.

Predictive models

Logistic regression was performed to determine if models combining shape analysis features could accurately screen aggressive meningioma.

Model 1 was built to predict WHO II-III meningioma from circularity, FD and NSB. Model 2 was built to predict brain parenchyma invasion from circularity, solidity and NSB.

Both models were cross-validated (k-fold cross-validation procedure with k=5). Variance inflation factor was calculated for each variable to control collinearity. Values ranged from 2.14 to 5.78 in Model 1 and from 2.25 to 6.32 in Model 2 suggesting a potential but not a serious collinearity problem.

Both models' equations and optimal thresholds are provided in **Table 3** along with diagnostic performances. Optimal thresholds and diagnostic performances of each independent variables used in these models are also presented. ROC curves are provided in **Figure 5**. AUC of Model 1 was 0.71 to predict WHO II-III meningioma. AUC of Model 2 was 0.72 to predict brain parenchyma invasion.

Visual analysis

Cohen's kappa was 0.64. Both raters achieved very similar diagnostic performances. Diagnostic performances after consensus between the two readers are provided in **Table 3**.

IV – Discussion

Main results

This study highlights the ability of shape analysis to predict brain parenchyma invasion and higher WHO grade in supratentorial meningioma. Low circularity and solidity ; high FD, NSB and RSL were associated with both WHO II-III meningioma and brain parenchyma invasion. Cross-validated models have an AUC > 0.70 (acceptable for a diagnostic test[20]) in predicting WHO II-III and brain invasive meningioma. Moreover, shape analysis outperforms standard visual analysis in predicting aggressive meningioma and appears more reproducible with ICC indicating an excellent inter-rater agreement. With appropriate thresholds, shape analysis features can exclude brain invasive meningiomas with NPV > 0.95.

Brain parenchyma invasion prediction

Brain invasion is not only a major criterion used by pathologists to grade meningioma according to WHO classification, but also a crucial element that has to be taken in account by the neurosurgeon[2,5]. Several reasons support the importance of its assessment in MRI. Brain invasion influences the surgical technique[2] all the more as invasive meningioma are less cleavable[21]. It has a prognostic significance as invasive meningioma are more prone to recurrence[5]. Finally, invasion may not be detected in histopathology due to a lack of tissue sample[2,5].

To date conventional MRI biomarkers cannot predict reliably brain invasion[5] even though radiomics models recently achieved interesting diagnostic performances[2,7]. Radiomics models suffer however from their complexity and lack of reproducibility which is slowing down their adoption in daily practice[22]. Our work, focusing only on shape features, has not only acceptable performances but also a simpler approach which might facilitate its translatability to daily practice.

WHO II-III prediction

Deep-learning and radiomics models have recently achieved impressive performances in the detection of WHO II-III meningioma[11,23]. The “black box” effect in deep learning as well as the inclusion of non-shape features in radiomics models makes these study hard to connect to our work.

Prior studies already reported that aggressive meningioma (WHO II-III) tend to have more complex and irregular shapes[1,4]. Coroller et al.[1] explored spherical disproportion which estimates the degree of deviation of an object from a sphere (similarly as circularity reflects the deviation from a circle). They identified a significant association between spherical disproportion and WHO II-III meningioma (AUC : 0.61). Yan et al.[4] performed a more extensive shape analysis using three shape parameters : vertical Feret’s diameter, perimeter over convex perimeter (similar to solidity) and skeleton’s length over the area (similar to RSL). They also found an association between these elements and WHO II-III meningioma. Therefore, our results appear concordant with these works.

Two prior studies[3,24] have examined the association between fractal analysis features and tumor grade. Nevertheless, the authors used this technique differently as they considered FD as a marker of tumoral enhancement heterogeneity. The present work provides a new way to use fractal analysis. FD in this study measures the outline’s complexity at different scales.

Limitations

This work is limited by its retrospective nature and the limited number of subjects relative to a single center study. WHO II-III meningioma are over-represented as our studied population consists of patients who underwent surgery.

We cannot exclude that the use of two different MRI systems affected the results of shape analysis. We argue that our choice of bicubic interpolation as rescaling method minimized the differences between the two systems.

Also, our cross-validated models have slightly lower AUC in predicting aggressive meningioma than previous radiomics or deep-learning studies [2,7,11]. This supports the necessity to consider other imaging biomarkers alongside shape features.

Currently, the post-processing is time-consuming and cannot be used in daily practice. Segmentation algorithms might allow an automatic selection of the appropriate slices and an extraction of the binarized tumoral shape. The next steps could be easily automatized as they rely on well-established algorithms.

V – Conclusions

MRI shape analysis is a potentially informative tool to predict histological higher WHO grade and brain invasion in case of supratentorial meningioma. Further prospective studies including the evaluation of a fully-automatized and totally reproducible process are required to confirm the results.

VI - Acknowledgments

We have no Conflict of Interest.

VII - References

- [1] Coroller TP, Bi WL, Huynh E, Abedalthagafi M, Aizer AA, Greenwald NF, et al. Radiographic prediction of meningioma grade by semantic and radiomic features. *PloS One* 2017;12:e0187908. <https://doi.org/10.1371/journal.pone.0187908>.
- [2] Zhang J, Yao K, Liu P, Liu Z, Han T, Zhao Z, et al. A radiomics model for preoperative prediction of brain invasion in meningioma non-invasively based on MRI: A multicentre study. *EBioMedicine* 2020;58:102933. <https://doi.org/10.1016/j.ebiom.2020.102933>.
- [3] Czyz M, Radwan H, Li JY, Filippi CG, Tykocki T, Schulder M. Fractal Analysis May Improve the Preoperative Identification of Atypical Meningiomas. *Neurosurgery* 2017;80:300–8. <https://doi.org/10.1093/neuros/nyw030>.
- [4] Yan P-F, Yan L, Hu T-T, Xiao D-D, Zhang Z, Zhao H-Y, et al. The Potential Value of Preoperative MRI Texture and Shape Analysis in Grading Meningiomas: A Preliminary Investigation. *Transl Oncol* 2017;10:570–7. <https://doi.org/10.1016/j.tranon.2017.04.006>.
- [5] Brokinkel B, Hess K, Mawrin C. Brain invasion in meningiomas-clinical considerations and impact of neuropathological evaluation: a systematic review. *Neuro-Oncol* 2017;19:1298–307. <https://doi.org/10.1093/neuonc/nox071>.
- [6] Liu Y, Chotai S, Chen M, Jin S, Qi S, Pan J. Preoperative Radiologic Classification of Convexity Meningioma to Predict the Survival and Aggressive Meningioma Behavior. *PLOS ONE* 2015;10:e0118908. <https://doi.org/10.1371/journal.pone.0118908>.
- [7] Kandemirli SG, Chopra S, Priya S, Ward C, Locke T, Soni N, et al. Presurgical detection of brain invasion status in meningiomas based on first-order histogram based texture analysis of contrast enhanced imaging. *Clin Neurol Neurosurg* 2020;198:106205. <https://doi.org/10.1016/j.clineuro.2020.106205>.
- [8] Hale AT, Wang L, Strother MK, Chambless LB. Differentiating meningioma grade by imaging features on magnetic resonance imaging. *J Clin Neurosci Off J Neurosurg Soc Australas* 2018;48:71–5. <https://doi.org/10.1016/j.jocn.2017.11.013>.
- [9] Hashiba T, Hashimoto N, Maruno M, Izumoto S, Suzuki T, Kagawa N, et al. Scoring radiologic characteristics to predict proliferative potential in meningiomas. *Brain Tumor Pathol* 2006;23:49–54. <https://doi.org/10.1007/s10014-006-0199-4>.
- [10] Li H, Zhao M, Wang S, Cao Y, Zhao J. Prediction of pediatric meningioma recurrence by preoperative MRI assessment. *Neurosurg Rev* 2016;39:663–9. <https://doi.org/10.1007/s10143-016-0716-9>.
- [11] Hu J, Zhao Y, Li M, Liu J, Wang F, Weng Q, et al. Machine learning-based radiomics analysis in predicting the meningioma grade using multiparametric MRI. *Eur J Radiol* 2020;131:109251. <https://doi.org/10.1016/j.ejrad.2020.109251>.

- [12] Schneider CA, Rasband WS, Eliceiri KW. NIH Image to ImageJ: 25 years of image analysis. *Nat Methods* 2012;9:671–5.
- [13] Parker J, Kenyon RV, Troxel DE. Comparison of interpolating methods for image resampling. *IEEE Trans Med Imaging* 1983;2:31–9. <https://doi.org/10.1109/TMI.1983.4307610>.
- [14] Wang H, Dong Y. An improved image segmentation algorithm based on Otsu method. In: Zhou L, editor., Beijing, China: 2007, p. 66250I. <https://doi.org/10.1117/12.790781>.
- [15] Ahammer H, DeVaney TTJ. The influence of edge detection algorithms on the estimation of the fractal dimension of binary digital images. *Chaos Woodbury N* 2004;14:183–8. <https://doi.org/10.1063/1.1638947>.
- [16] A. Karperien, “FracLac for Image J, version 2.5,” <http://rsb.info.nih.gov/ij/plugins/fraclac/FLHelp/Introduction.htm> (1999–2012). n.d.
- [17] Reiss MA, Sabathiel N, Ahammer H. Noise dependency of algorithms for calculating fractal dimensions in digital images. *Chaos Solitons Fractals* 2015;78:39–46. <https://doi.org/10.1016/j.chaos.2015.07.004>.
- [18] Arganda-Carreras I, Fernández-González R, Muñoz-Barrutia A, Ortiz-De-Solorzano C. 3D reconstruction of histological sections: Application to mammary gland tissue. *Microsc Res Tech* 2010;73:1019–29. <https://doi.org/10.1002/jemt.20829>.
- [19] Backer-Grøndahl T, Moen BH, Arnli MB, Torseth K, Torp SH. Immunohistochemical characterization of brain-invasive meningiomas. *Int J Clin Exp Pathol* 2014;7:7206–19.
- [20] Mandrekar JN. Receiver operating characteristic curve in diagnostic test assessment. *J Thorac Oncol Off Publ Int Assoc Study Lung Cancer* 2010;5:1315–6. <https://doi.org/10.1097/JTO.0b013e3181ec173d>.
- [21] Pizem J, Velnar T, Prestor B, Mlakar J, Popovic M. Brain invasion assessability in meningiomas is related to meningioma size and grade, and can be improved by extensive sampling of the surgically removed meningioma specimen. *Clin Neuropathol* 2014;33:354–63. <https://doi.org/10.5414/NP300750>.
- [22] Gillies RJ, Kinahan PE, Hricak H. Radiomics: Images Are More than Pictures, They Are Data. *Radiology* 2016;278:563–77. <https://doi.org/10.1148/radiol.2015151169>.
- [23] Zhang H, Mo J, Jiang H, Li Z, Hu W, Zhang C, et al. Deep Learning Model for the Automated Detection and Histopathological Prediction of Meningioma. *Neuroinformatics* 2020. <https://doi.org/10.1007/s12021-020-09492-6>.
- [24] Kim S, Park YW, Park SH, Ahn SS, Chang JH, Kim SH, et al. Comparison of Diagnostic Performance of Two-Dimensional and Three-Dimensional Fractal Dimension and Lacunarity Analyses for Predicting the Meningioma Grade. *Brain Tumor Res Treat* 2020;8:36. <https://doi.org/10.14791/btrt.2020.8.e3>.

VIII – Tables and Figures

Table 1 : Studied population and parameters.

Studied parameters		Studied population	
Shape analysis		Sex ratio (M/F)	0.51 (34 vs. 67)
Circularity	$4 \cdot \pi \cdot (\text{area} / \text{perimeter}^2)$	Age (y)	60.2 (SD: 14.5)
Aspect ratio	major axis / minor axis	Size (mm)	51.0 (SD : 16.4)
Solidity	area/convex area	Location (%)	
Fractal analysis		Convexity	35.6 (36/101)
Fractal dimension	box counting method	Parasagittal	25.7 (26/101)
Skeleton analysis		Falx	5.0 (5/101)
Number of skeleton's branches (NSB)	number of branches needed to build the skeleton	Olfactive groove	11.9 (12/101)
Relative skeleton length (RSL)	skeleton length / (major axis + minor axis)	Sphenoidal ridge	12.9 (13/101)
		Skull base (other)	8.9 (9/101)
		WHO II-III (%)	38.6 (39/101)

Table 2 : Results of shape and fractal analysis

	No brain invasion	Brain invasion	P-value
Circularity	0.689 [0.533 – 0.844]	0.609 [0.430 – 0.788]	0.0016
Solidity	0.931 [0.867 – 0.994]	0.899 [0.849 – 0.950]	0.00038
Aspect ratio	1.343 [0.952 – 1.735]	1.314 [0.926 – 1.701]	0.397
FD	1.121 [1.091 – 1.153]	1.136 [1.093 – 1.179]	0.0079
NBS	8.011 [1 – 17.605]	13.923 [1 – 17.719]	0.0027
RSL	0.621 [0 – 1.3236]	0.9263 [1 – 2.2230]	0.0194

	WHO I	WHO II-III	P-value
Circularity	0.705 [0.583 – 0.827]	0.638 [0.439 – 0.838]	0.00029
Solidity	0.935 [0.883 – 0.986]	0.917 [0.839 – 0.995]	0.0149
Aspect ratio	1.308 [1.095 – 1.521]	1.389 [0.883 – 1.850]	0.183
FD	1.118 [1.095 – 1.142]	1.131 [1.090 – 1.173]	0.00059
NBS	7.484 [1 – 12.092]	10.769 [1 – 24.538]	0.0040
RSL	0.568 [0 – 1.103]	0.808 [0 – 1.888]	0.0177

Values are means and 95 % confidence intervals ; statistical test for p-value : Mann-Whitney.

Table 3 : Predictive models

Predictors of WHO II-III meningioma

	Threshold	Se	Sp	PPV	NPV	Acc
Circularity	< 0.641	0.539	0.871	0.724	0.750	0.743
FD	> 1.129	0.629	0.855	0.710	0.803	0.773
NBS	> 9.5	0.487	0.823	0.633	0.718	0.693
Model 1	0.438	0.615	0.807	0.667	0.769	0.733
Visual	-	0.346	0.871	0.627	0.679	0.668

Predictors of brain invasion

	Threshold	Se	Sp	PPV	NPV	Acc
Circularity	< 0.657	0.846	0.705	0.297	0.969	0.723
Solidity	< 0.910	0.769	0.818	0.385	0.960	0.812
NBS	> 10	0.750	0.841	0.391	0.961	0.830
Model 2	> 0.152	0.692	0.864	0.429	0.950	0.842
Visual	-	0.614	0.846	0.372	0.937	0.817

*Model 1 : $Logit(p) = -18.1627 - (8.1407 * Circularity) + (20.7501 * FD) - (0.0142 * NBS)$*

*Model 2 : $Logit(p) = 5.5092 - (1.0224 * Circularity) - (8.4289 * Solidity) + (0.098 * NBS)$*

Figure 1 :

Standard process of binarization.

Figure 2 :

Box counting method. Outlines have been thickened for the illustrative purpose.

Figure 3 :

Examples of topological skeletons. Outlines in white and skeletons in orange have been thickened for the illustrative purpose.

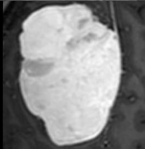
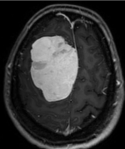
Figure 4 : Representative images

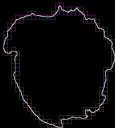
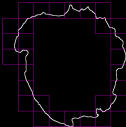
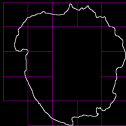
A: "regular-shaped" meningioma with high circularity (0.743), high solidity (0.960), low number of branches (3) and low relative skeleton's length (0.41). WHO I meningioma.

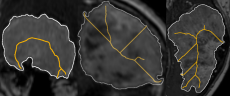
B : "irregular-shaped" meningioma with low circularity (0.373), low solidity (0.835), high number of branches (20) and high relative skeleton's length (2.03). WHO II meningioma.

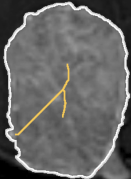
Figure 5 : ROC curves

ROC curves with AUC showing the ability of our features to predict WHO II-III meningioma and brain parenchyma invasion. X-axis is false positive rate and Y-axis is true positive rate.

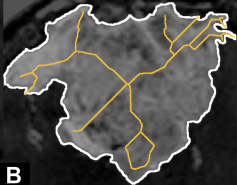






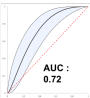


A

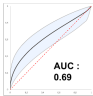


B

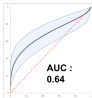
WHO II – III



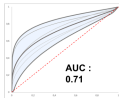
Circularity



Fract. dim.

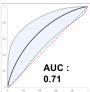


NoB.

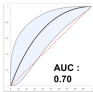


Combined

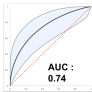
Brain invasion



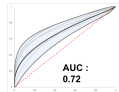
Circularity



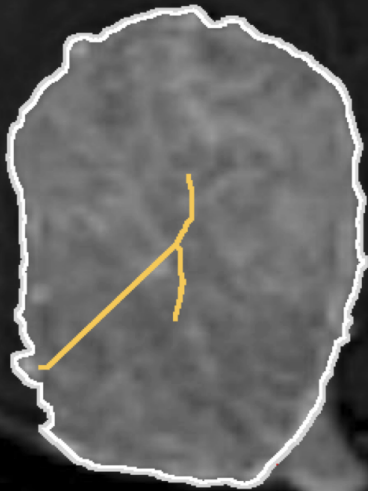
Sol.



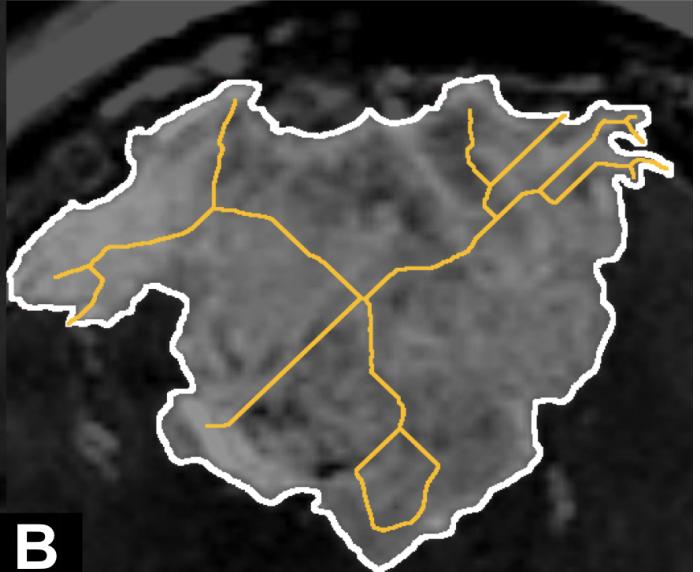
NoB.



Combined



A



B

Extraction of shape analysis features

(circularity, solidity, fractal analysis, topological skeleton)



Regular-shaped meningioma

(high circularity and solidity,
simple topological skeleton)



WHO I meningioma

Irregular-shaped meningioma

(low circularity and solidity,
complex topological skeleton)



WHO II-III meningioma